

# Incorporating Breaking Wave Predictions in Spectral Wave Forecast Models

Michael Banner and Russel Morison

School of Mathematics, The University of New South Wales, Sydney 2052, Australia

Email: [m.banner@unsw.edu.au](mailto:m.banner@unsw.edu.au), Tel: 612-9385-7072, Fax: 612-9385-7123

## 1. Introduction

Dissipation through wave breaking is a key process in the evolution of wind waves. Most of the wind input momentum and energy fluxes to the waves leave the wave field locally via wave breaking to drive currents and generate turbulence, respectively, in the upper ocean (Donelan, 1998).

Wave breaking underlies the very significant enhancement in surface layer turbulent kinetic energy (TKE) dissipation rate measurements over conventional rough wall levels (e.g. Terray et al., 1996, Gemmrich and Farmer, 2004). Wave breaking also enhances interfacial fluxes through enhanced overturning of the sea surface (e.g. Melville, 1994). Recent basin-wide theoretical model studies have demonstrated the potentially strong contributions from breaking waves to the circulation and mixing (e.g. Restrepo, 2007, among others).

Yet, in wave forecasting models, the dissipation rate remains the least well-understood source term relative to the other two source terms, wind input and nonlinear spectral transfer, and these models do not provide any breaking predictions.

While incompletely understood, evidence is building that wave breaking in deep water is a process with a generic threshold that reflects the convergence rate and geometrical steepening of the waves that break. From their innovative analysis of storm waves, Banner et al. (2002) reported that a parameter based on the wave spectral saturation (Phillips, 1985) provides a robust spectral breaking threshold, at least for waves in the energy-containing range. Background turbulence in the wave boundary layer, to which breaking waves of all scales contribute, also has a role in dissipating the energy of wind waves.

The present contribution outlines a methodology that synthesises several aspects of recent progress on wave breaking. Here we report on an initial validation of predictions for the dominant wind waves against data from the recent FAIRS experiment, and present model breaking predictions as the wave age is varied, for wind speeds from light to hurricane strength.

## 2. Modeling background

Phillips (1985) introduced  $\Lambda(\mathbf{c})$ , the spectral density of breaking crest length per unit sea surface area as a basic spectral measure of wave breaking, as described in the following paragraph. Recent advances in observational techniques have facilitated initial field measurements of  $\Lambda(\mathbf{c})$ , a challenging task over the open ocean.

The spectral measure of breaking waves,  $\Lambda(\mathbf{c})$ , has the property that  $\Lambda(\mathbf{c}) d\mathbf{c}$  gives the crest length/unit sea surface area, of breaking crests travelling with velocities in  $(\mathbf{c}, \mathbf{c}+d\mathbf{c})$ .  $\Lambda(\mathbf{c})$  is one of the primary breaking forecast parameters computed in this study.  $\Lambda(\mathbf{c})$  can also be used to model breaking wave enhancements to the wind stress and allied air-sea fluxes such as sea spray based on the sea state, rather than the wind field.

It is noted that the limited open ocean data for  $\Lambda(c)$  reported to date do not provide an unambiguous trend towards shorter scales, as discussed below. The image processing techniques used by various authors are quite distinct, and we were not able to reconcile the reported differences. Hence in this study while breaking occurs across the spectrum, we decided to focus initially on predicting the breaking of the waves at the spectral peak. These dominant waves are likely the most energetic breaking wave scale in growing seas, as well as in very severe sea states where they are strongly forced by the wind.

A closely related major challenge is to be able to relate the geometric/kinematic measurements of  $\Lambda(c)$  accurately to the underlying energy dissipation rate  $\varepsilon(c)$ . Phillips (1985, equation (6.3)) proposed the following connection between these two distributions, given below in scalar form:

$$\varepsilon(c) dc = b g^{-1} c^5 \Lambda(c) dc \quad (1)$$

where the non-dimensional coefficient  $b$  connects the energetics to the whitecap geometry and kinematics, and reflects the breaking strength.

Underlying (1) is the assumption that the mean wave energy dissipation rate at scale  $(c, c+dc)$  is dominated by wave breaking at that scale. This may have shortcomings, especially for shorter breaking waves due to the attenuation of short wave energy by the passage of longer breaking waves (e.g. Banner et al., 1989).

A less restrictive form for  $S_{ds}$  should have a local contribution from the given breaking wave scale,  $S_{ds}^{loc}$ , plus a background attenuation component,  $S_{ds}^{nloc}$ , representing the background turbulence in the wave boundary layer and the cumulative attenuation of short waves by longer breaking waves sweeping through them. To account for these effects, Banner and Morison (2006) modeled the total dissipation rate as the sum of these two contributions:

$$S_{ds} = S_{ds}^{loc} + S_{ds}^{nloc} \quad (2)$$

and used  $S_{ds}^{loc}$  as the appropriate dissipation rate in (1).

The dependence of breaking strength  $b$  on wave variables is not well understood. One would expect that  $b$  should increase systematically with wave nonlinearity (steepness). Banner and Peirson (2007) reported direct measurements of  $b$  values for narrow-band laboratory spilling breakers that increase linearly from  $8 \times 10^{-5}$  to  $1.2 \times 10^{-3}$  as the mean wave steepness increased. The very recent laboratory study of Tian et al. (2008) also reported a similar trend for  $b$ .

Initial field measurements of  $\Lambda$  and  $b$  were published by Phillips et al. (2001) and Melville and Matusov (2002). These were gathered only during fully developed sea states, and also had issues with their data processing. For model validation, data for growing seas as well as developed wind seas were needed. The only available data was from the FAIRS project from RV FLIP in 2000. More data is becoming available, including data from our ONR RaDyO project collected in 2008 and 2009. This is being analyzed for  $\Lambda(c)$  and  $b$  to add further data sets for model refinement.

The FAIRS data was analysed by Gemmrich et al. (2008) to produce measurements of  $\Lambda(c)$  and the mean breaking strength  $\langle b \rangle$  averaged across the wave spectrum. While the range

of wave age conditions is rather limited, these results provide a valuable initial validation source for our model performance.

### 3. Recent comprehensive wave breaking field observations

#### 3.1 Breaking probability in the spectrum

Banner et al. (2000) found a significant correlation for the breaking probability of the dominant wind waves with the significant wave steepness, operative once a threshold significant steepness level had been exceeded. In our spectral breaking wave forecast model framework, a breaking criterion also applicable to waves shorter than the dominant waves was sought to be able to include breaking wave effects associated with shorter wave scales.

From their analysis of storm wave datasets, Banner et al. (2002) reported a high correlation of breaking probability with the spectral saturation  $B = k^4 \Phi(\mathbf{k}) = f^5 F(f)/2g^2$  for wave scales from the spectral peak frequency  $f_p$  out to  $2.5f_p$ , and demonstrated a very strong threshold behaviour. After normalization to allow for the growing directional spreading of the waves with  $f/f_p$ , they found that the saturation breaking threshold is almost constant across the above observed frequency range of  $1 < f/f_p < 2.5$ . This is seen in Fig. 7 in Banner et al. (2002). That result formed the basis of our formulation of the spectral wave breaking dissipation rate source term, which underpins our calculation of breaking crest length spectral density and breaking strength.

#### 3.2 Observational results from the FAIRS experiment

The data analysis methodology for the breaking crest spectral density distributions used to validate this study was reported in Gemmrich et al. (2008). In brief, the FAIRS experiment took place during September-October 2000 from the research platform FLIP, roughly 150 km off Monterey, California. Two downward looking monochrome video cameras mounted on the

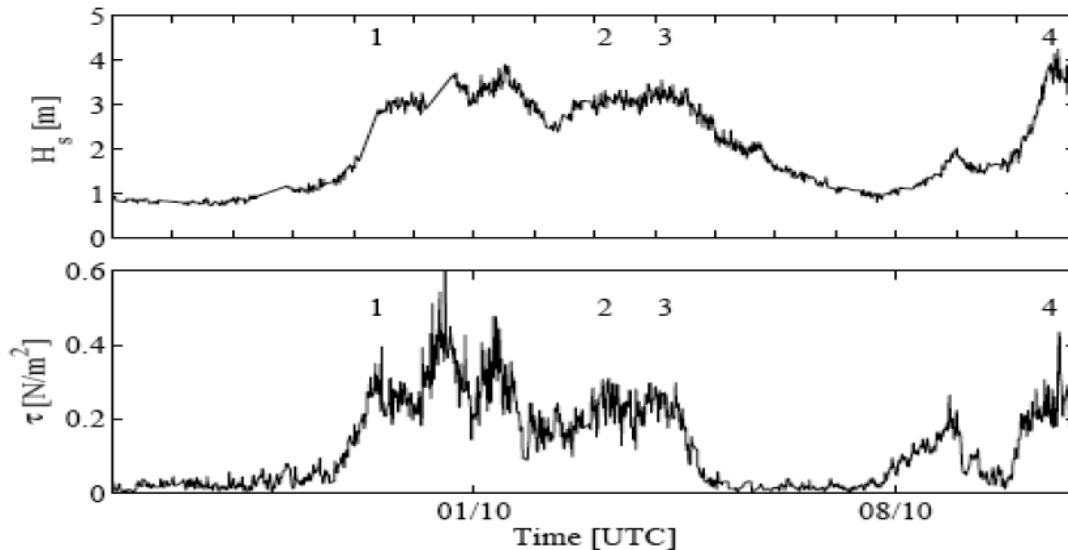


Figure 1. Significant wave height ( $H_s$ ) and wind stress ( $\tau$ ) during the FAIRS experiment. The wind direction was around  $300^\circ$  for most of the observational period. Periods 1 (growing seas) and 3 (mature seas) are of particular interest in this study, during which the mean wind was measured to be 12 m/s.

starboard boom recorded whitecap events. There were synchronous measurements of wind speed and direction, wind stress, wave height and energy dissipation rates. Fig. 1 summarises the observed conditions and salient data. This unique dataset includes wave breaking measurements for a developing wind seas ( $U_{10}/c_p \sim 1.09$ ), in addition to mature sea conditions ( $U_{10}/c_p \sim 0.81$ ). Such data for developing wind seas were not previously available. Here, developing sea ( $U_{10}/c_p \sim 1.09$ ) is denoted Period 1, and mature sea ( $U_{10}/c_p \sim 0.81$ ) is denoted Period 3. Also indicated in Fig.1 are Periods 2 and 4. These refer to aging seas and a newly developing mixed sea event during the FAIRS observational period, but were not used in the present study.

Fig. 2 summarises the differences in the measured probability distribution of breaking waves with wave speed histograms for developing seas ( $U_{10}/c_p \sim 1.09$ ) and mature seas ( $U_{10}/c_p \sim 0.81$ ). Note that for the *developing* seas (period 1), significant breaking occurs around the spectral peak, as well as for the shorter waves. However, there is no breaking of the waves at the peak

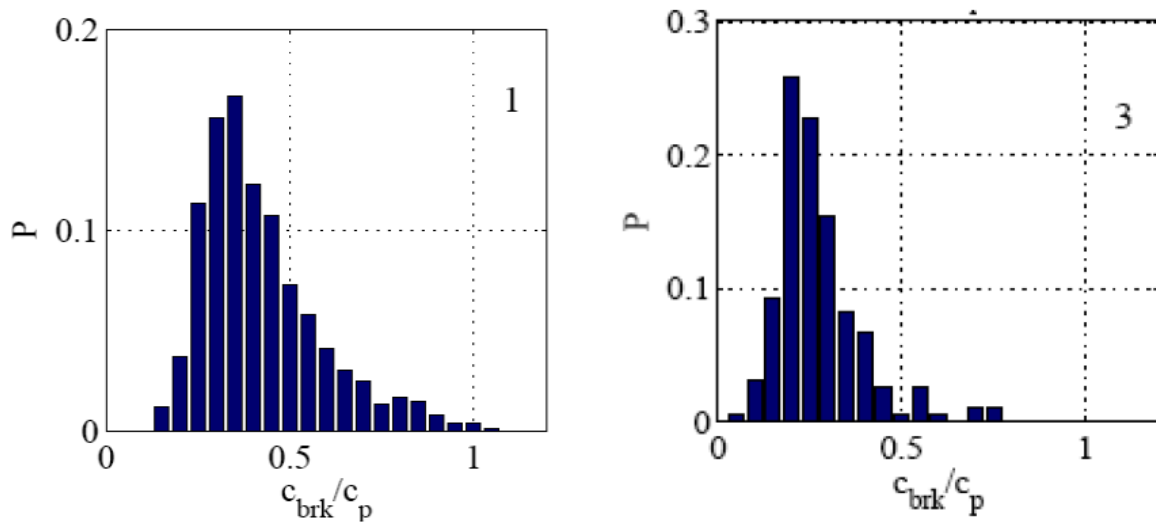


Figure 2. Probability distribution of breaking waves as a function of wave speed relative to the spectral peak wave speed, for period 1 (growing seas) and 3 (mature seas). Note that breaking is largely absent in the spectral peak region (approx. 0.7 to 1.3  $c_p$ ) for mature seas.

of the spectrum for the mature seas in Period 3. These observations confirm the presence of dominant wave breaking, as measured directly by the breaker speeds close to the dominant wave speed  $c_p$ . Hence these are not shorter waves that break at the crests of dominant waves.

This figure also indicates a pronounced fall-off in the breaking wave probability distribution as  $c_{brk}$  decreases below about  $\sim(0.2-0.3)c_p$ . This does not appear to be due to resolution limitations of the observations. As the underlying physics is not understood, we have focused our attention in this study on the dominant breaking waves, seeking to forecast their geometrical distribution and strength for different wind speed and wave age conditions. An extension to shorter breaking waves is underway utilizing data from our RaDyO project during 2008 and 2009.

#### 4. Brief description of the methodology

The breaking probability at scale  $c$  is based on the following framework proposed by Phillips (1985) : if  $\Lambda(c)$  is the spectral density of breaking wave crest length per unit area with velocities in the range  $(c, c+dc)$ , then the passage rate of breaking crests in  $(c, c+dc)$  past a fixed point is  $c\Lambda(c)dc$ .

The analogous concept of the spectral density of the total wave crest length per unit area  $\Pi(c)$  gives the *total* crest passage rate in  $(c, c + dc)$  past a fixed point as  $c\Pi(c)dc$ .

The breaking probability  $P_{br}(c_0)$  at a wave scale  $c_0$  is then defined as:

$$Pr_{br}(c_0) = \frac{\int c \Lambda dc}{\int c \Pi dc} \quad (3)$$

where each integration is over  $(c_0-dc/2, c_0+dc/2)$ , and  $dc \rightarrow 0$ . From dimensional and physical considerations, it can be shown that the denominator term yields

$$\Pi(c) = g/(2\pi c^3) \quad (4)$$

Integrating the first moment of (4) over a nominal  $\pm 30\%$  relative frequency bandwidth about the spectral peak gives

$$c_p \Pi(c_p) = \chi g / (1.32 \pi c_p^2) \quad (5)$$

where  $\chi \sim 0.6 \pm 0.05$  is the measured crest count factor, using the Riding Wave Removal technique (Banner et al., 2002).

Using this result in (3) gives

$$\Lambda(c_p) = (\chi g / 1.32 \pi c_p^3) * Pr(\tilde{\sigma}_p). \quad (6)$$

The sea state threshold variable used was the normalised spectral saturation

$$\tilde{\sigma}(k) = \sigma(k) / \langle \theta(k) \rangle \quad (7)$$

where  $\sigma(k)$  is the azimuth-integrated spectral saturation given by

$$\begin{aligned} \sigma(k) &= k^4 \Phi(k) \\ &= (2\pi)^4 f^5 G(f) / 2g^2 \end{aligned} \quad (8)$$

and  $\langle \theta(k) \rangle$  is the mean spectral spreading width given by

$$\langle \theta(k) \rangle = \int_{-\pi}^{\pi} (\theta - \bar{\theta}) F(k, \theta) k d\theta / \int_{-\pi}^{\pi} F(k, \theta) k d\theta \quad (9)$$

where  $\bar{\theta}$  is the mean wave direction, and  $F(k)$ ,  $G(f)$  and  $F(k,\theta)$  are, respectively, the spectra of wave height as a function of scalar wavenumber, frequency and vector wavenumber.

Using the spectral saturation normalized by the directional spreading defined above, Banner, Gemmrich and Farmer (2002) showed evidence for a common threshold behavior for the dissipation rate at different frequencies at and above the spectral peak. The form connecting breaking probability (as defined above) with the normalized saturation from a linear fit to the Banner et al (2002) results was

$$\text{Pr}_{\text{br}}(\tilde{\sigma}_p) = H(\tilde{\sigma} - \tilde{\sigma}_T) * \alpha_{\text{br}} * (\tilde{\sigma} - \tilde{\sigma}_T) \quad (10)$$

where  $\alpha_{\text{br}} \sim 33$ . In our methodology,  $\tilde{\sigma}(k)$  calculated from our spectral wave model is used to calculate the breaking probability for the spectral peak waves at any wave age  $c_p/U_{10}$ .

#### 4.1 Spectral Peak Breaking Strength Coefficient $b_p$

We begin by recalling Phillips (1985) form below that links the local spectral dissipation rate and breaking crest length spectral density. This is shown here for the spectral wave energy density that integrates to the mean square wave height.

$$S_{\text{ds}}^{\text{loc}}(c) dc = b g^{-2} c^5 \Lambda(c) dc \quad (11)$$

This is the term in (2) that is relevant to the local breaking strength and crest length properties. It should be noted that, a priori,  $b$  may vary across the spectrum.

For the spectral peak, using the preceding result for  $\Lambda(c)$  and transforming the local dissipation rate from  $c$  to  $k$  dependence to match with our wave model output, we obtain

$$\begin{aligned} b_p &= 2 \frac{g^3}{c_p^8} \frac{S_{\text{ds}}^{\text{loc}}(k_p)}{\Lambda(c_p)} \\ &= \frac{2.64\pi}{\chi} \frac{g^2}{c_p^5} \frac{S_{\text{ds}}^{\text{loc}}(k_p)}{\text{Pr}_{\text{br}}(\tilde{\sigma}_p)} \end{aligned} \quad (12)$$

Recalling (6) :

$$\Lambda(c_p) = (\chi g/1.32\pi c_p^3) * \text{Pr}(\tilde{\sigma}_p).$$

it is seen that with the wave model output for the spectrum (for  $\tilde{\sigma}$ ) and the local component of the dissipation rate source term ( $S_{\text{ds}}^{\text{loc}}$ ), equations (6) and (12) provide the breaking crest length spectral density and breaking strength at the spectral peak at any time step.

## 5. Results

The spectral wind wave model used to generate the present results is described in detail in Banner and Morison (2009). The source terms in that model have been developed as refinements of previously reported forms. The wind input term is essentially the Janssen (1991) form with sheltering introduced in the spectral tail. Its calculated drag coefficients are very

close to those observed. The nonlinear transfer term is the Exact NL implementation of Tracy and Resio (1982) extended to  $\pm 180$  degrees. The dissipation rate source term is a refinement of the form described in Banner and Morison (2006). The hallmark of this source term combination is that it provides accurate model forecasts of all observable parameters, for both the large and small-scale waves, over a very wide wind speed range from light to hurricane conditions. The major advance in our approach is that the spectral balance of wind input and dissipation source terms allows for sufficient wind input to the spectral peak waves be able to generate their observed breaking levels at during developing wind seas.

### 5.1 Validation against the FAIRS data

In Fig. 3 it can be seen that the modeled value of  $\Lambda(c_p)$  agrees well with the measurements for Period 1. There was no breaking observed at the spectral peak for the mature sea (Period 3), which the model also reproduced.

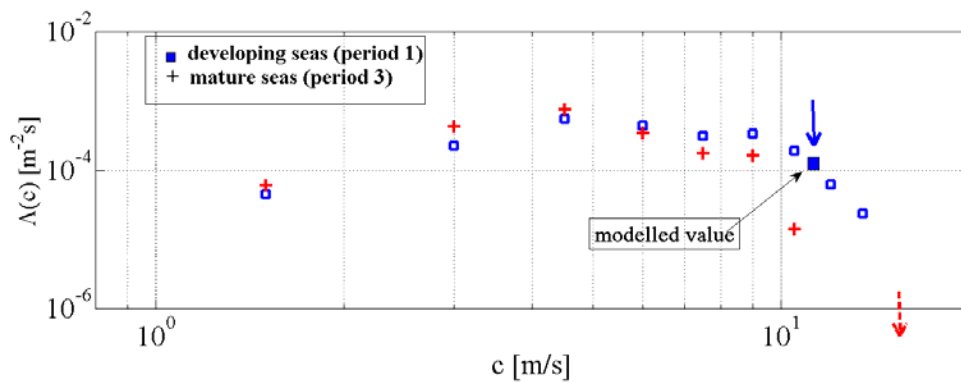


Fig. 3 Calculated  $\Lambda(c_p)$  plotted on the measure  $\Lambda(c)$  spectra for the developing (period 1) and mature (period 3) sea states in FAIRS. The corresponding wave ages were  $c_p/U_{10} \sim 0.9$  and 1.25 respectively, with the nominal wind speed  $U_{10} \sim 12$  m/s.

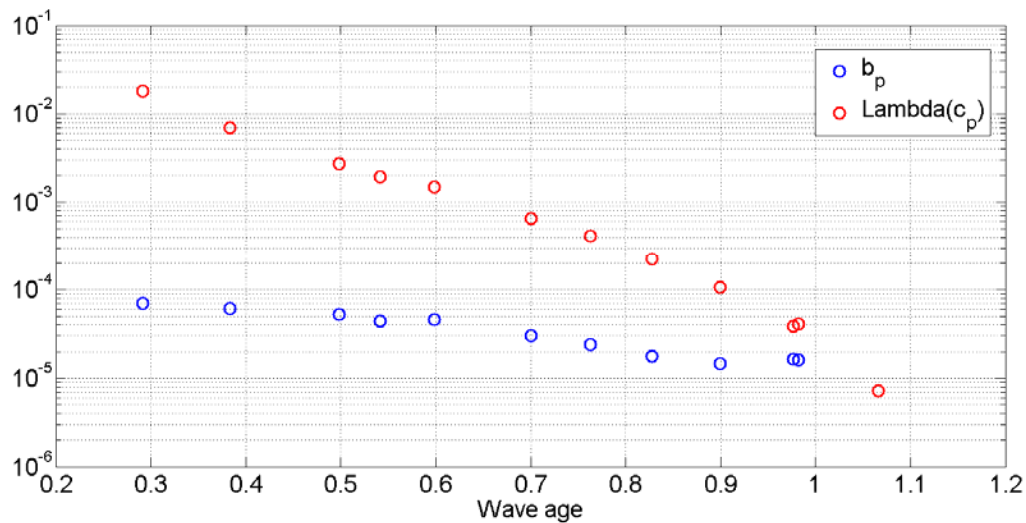


Figure 4. Predicted variation of  $\Lambda(c_p)$  and  $b_p$  with wave age  $c_p/U_{10}$  for the spectral peak waves for  $U_{10} = 12$  m/s.

Fig. 4 shows the modeled variation of the spectral peak lambda [ $\Lambda(c_p)$ ] and corresponding spectral peak breaking strength [ $b_p$ ] as the wave age  $c_p/U_{10}$  varies from young to old, for the wind speed  $U_{10}=12$  m/s representative of FAIRS. This figure shows that the predicted lambda and breaking strength levels *for the spectral peak waves* both decrease significantly with wave age, with the lambda level showing a larger dynamic range. The scatter seen is associated with instances where the spectral peak did not coincide closely with a grid point at the time chosen to display the values.

Unfortunately, there are no observed values of  $b_p$  presently available from measurements with which to compare the predicted level of  $b_p$ . The only observational estimates of breaking strength are the mean breaking strength  $\langle b \rangle$  which assumes that the breaking strength in (10) has a constant value across the spectrum. For period 1, Gemmrich et al. (2008) reported values of  $\langle b \rangle \sim 4 \times 10^{-5}$ . Therefore while a direct intercomparison is not possible at this time, the predicted level  $b_p$  for the spectral peak region has the same order of magnitude as  $\langle b \rangle$ .

### 5.2 Predicted variation of $\Lambda(c_p)$ and $b_p$ for different wind speed and wave age conditions

It is of fundamental interest to know how  $\Lambda(c)$  and  $b$  vary with wind speed over a wide range of conditions. To make initial progress, we calculated the predicted variation of the spectral peak values  $\Lambda(c_p)$  and  $b_p$  for wind speeds  $U_{10}$  of 12 m/s, 24 m/s and 48 m/s. These results are plotted in Figs 5 and 6.

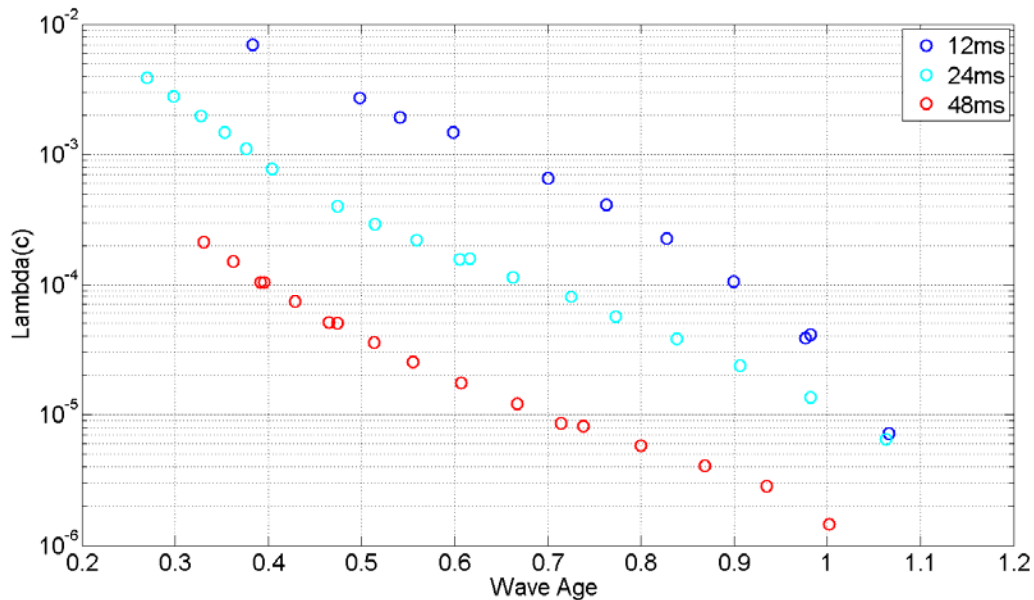


Figure 5. Predicted variation of  $\Lambda(c_p)$  with wave age for the spectral peak waves for  $U_{10} = 12$  m/s, 24 m/s and 48 m/s.



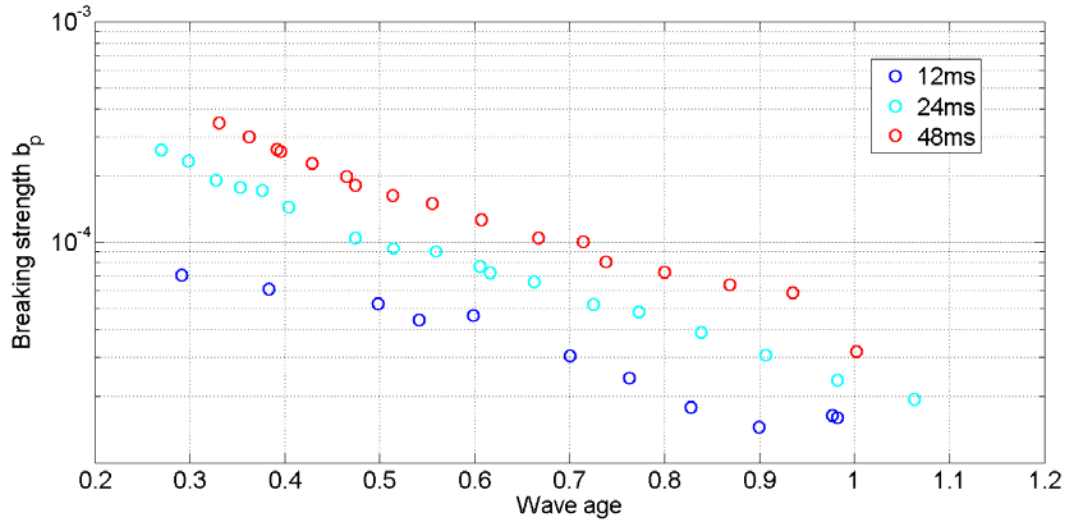


Figure 6. Predicted variation of corresponding  $b_p$  levels with wave age for the spectral peak waves for  $U_{10} = 12$  m/s, 24 m/s and 48 m/s

It is seen that as the wind speed increases for any wave age, the level of  $\Lambda(c_p)$  reduces significantly, while the breaking strength  $b_p$  is raised. The strong variation with wave age is seen at each wind speed.

Ongoing efforts are aimed at extending this work to be able to provide accurate breaking forecasts for shorter breaking waves.

## 5. Summary of Conclusions

- (i) our framework provides predictions of dominant wave breaking properties (crest length spectral density per unit area and breaking strength) using standard wave model output.
- (ii) it provides predictions consistent with the limited breaking data available for developing and mature wind seas.
- (iii) further validation against data is needed and will be made as suitable new breaking wave data sets as they become available.
- (iv) after further validation, this methodology can be easily added to existing spectral wave forecasting models. However, refinement of the nonlinear transfer source term beyond the DIA approximation is probably needed.

## Acknowledgements

The authors gratefully acknowledge the support of ONR for their air-sea interaction studies under the CBLAST and RaDyO DRI programs.

## References

- Banner, M.L., I.S.F Jones and J.C. Trinder, 1989: Wavenumber spectra of short gravity waves. *J. Fluid Mech.* 198, 321-344.
- Banner, M.L., J.R. Gemmrich and D.M. Farmer, 2002: Multiscale measurements of ocean wave breaking probability. *J. Phys. Oceanogr.*, 32, 3364-3375.
- Michael L. Banner and Russel P. Morison, 2006: On Modeling Spectral Dissipation due to Wave Breaking for Ocean Wind Waves. Proc. 9<sup>th</sup> International Workshop On Wave Hindcasting and Forecasting, Victoria, B.C., Canada, September 24-29, 2006
- Banner, M.L. and R.P. Morison, 2009: Refined source terms in wind wave models with explicit wave breaking forecasts. Part I. Model framework and validation against field data. Submitted to *Ocean Modelling*.
- Banner, M.L. and W.L. Peirson, 2007: Wave breaking onset and strength for two-dimensional deep water waves. *J. Fluid Mech.*, 585, 93-115.
- Donelan, M.A., 1998: Air-water exchange processes. In *Physical Processes in Oceans and Lakes* (J. Imberger, Ed), AGU Coastal and Estuarine Studies 54, 19-36.
- Gemmrich, J. R. and D.M. Farmer, 2004: Near-surface turbulence in the presence of breaking waves. *J. Phys. Oceanogr.*, 34, 1067-1086.
- Gemmrich, J.R., M.L. Banner, M.L. & C. Garrett, 2008: Spectrally resolved energy dissipation and momentum flux of breaking waves. *J. Phys. Oceanogr.*, 38, 1296-1312.
- Janssen, P.A.E.M., 1991: Quasi-linear theory of wind-wave generation applied to wave forecasting. *J. Phys. Oceanogr.*, 21, 1631-1642.
- Komen, G.J., L. Cavaleri, M.A. Donelan, K. Hasselmann, S. Hasselmann, and P.A.E.M. Janssen, 1994: *Dynamics and Modelling of Ocean Waves*, Cambridge University Press, Cambridge, 532pp.
- Melville, W.K. and P. Matusov, 2002: Distribution of breaking waves at the ocean surface. *Nature*, 417, 58-63.
- Melville, W.K., 1994: Energy dissipation by breaking waves. *J. Phys. Oceanogr.*, 24, 2041-2049.
- Phillips, O.M., 1985: Spectral and statistical properties of the equilibrium range in wind-generated gravity waves. *J. Fluid Mech.*, 156, 505-531.
- Phillips, O. M., F.L. Posner and J.P. Hansen, 2001: High resolution radar measurements of the speed distribution of breaking events in wind-generated ocean waves. surface impulse and wave energy dissipation rates. *J. Phys. Oceanogr.*, 31, 450-460.
- Resio, D., and W. Perrie, 2008: A two-scale approximation for efficient representation of nonlinear energy transfers in a wind wave spectrum. Part 1: Theoretical Development, *J. Phys. Oceanogr.* 38 (12) (2008), pp. 2801-2816.
- Restrepo, J. M., 2007: Wave Breaking Dissipation in a Wave-driven Circulation, *Journal of Physical Oceanography*, 37, 1749-1763.

Terray, E.A., M.A. Donelan, Y.C. Agrawal, W.M. Drennan, K.K. Kahma, A.J. Williams III, P.A. Hwang, and S.A. Kitaigorodskii, 1996: Estimates of kinetic energy dissipation under breaking waves. *J. Phys. Oceanogr.*, 26, 792-807.

Tian, Z, M. Perlin & W. Choi, 2008: Evaluation of a deep-water breaking criterion. *Phys. Fluids* 20, 066604. DOI: 10.1063/1.2939396

Tracy, B.A. and D.T. Resio, 1982: Theory and calculation of the nonlinear energy transfer between sea waves in deep water, WIS Rept 11, US Army Engineers Waterway Experiment Station.